Intratumoral administration of the immunologic adjuvant AS01$_B$ in combination with autologous CD1c (BDCA-1)$^+$/CD141 (BDCA-3)$^+$ myeloid dendritic cells plus ipilimumab and intravenous nivolumab in patients with refractory advanced melanoma

Jens Tijtgat [ID] ,[1] Xenia Geeraerts,[1] Anais Boisson,[2] Latoya Stevens,[1] Manon Vounckx,[1] Iris Dirven,[1] Julia Katharina Schwarze [ID] ,[1] Steven Raeymaeckers,[3] Ramses Forsyth,[4] Ivan Van Riet,[5] Sandra Tuyaerts [ID] ,[1] Karen Willard-Gallo,[2] Bart Neyns [ID] [1]

Correspondence to
Dr Bart Neyns;
bart.neyns@uzbrussel.be

ABSTRACT

Background Patients with advanced melanoma who progress after treatment with immune checkpoint-inhibitors (ICI) and BRAF-/MEK-inhibitors (if *BRAF*^{V600} mutated) have no remaining effective treatment options. The presence of CD1c (BDCA-1)$^+$ and CD141 (BDCA-3)$^+$ myeloid dendritic cells (myDC) in the tumor microenvironment correlates with pre-existing immune recognition and responsiveness to immune checkpoint blockade. The synthetic saponin-based immune adjuvant AS01$_B$ enhances adaptive immunity through the involvement of myDC.

Methods In this first-in-human phase I clinical trial, patients with metastatic melanoma refractory to ICI and BRAF-/MEK inhibitors (when indicated) were recruited. Patients received an intravenous administration of low-dose nivolumab (10 mg, every 2 weeks) plus an intratumoral (IT) administration of 10 mg ipilimumab and 50 µg (0.5 mL) AS01$_B$ (every 2 weeks). All myDC, isolated from blood, were injected on day 2 into the same metastatic lesion. Tumor biopsies and blood samples were collected at baseline and repeatedly on treatment. Multiplex immunohistochemistry (mIHC) was performed on biopsy sections to characterize and quantify the IT and peritumoral immune cell composition.

Results Study treatment was feasible and well tolerated without the occurrence of unexpected adverse events in all eight patients. Four patients (50%) obtained a complete response (CR) in the injected lesions. Of these, two patients obtained an overall CR, and one patient a partial response. All responses are ongoing after more than 1 year of follow-up. One additional patient had a stable disease as best response. The disease control rate was 50%. Median progression-free survival and overall survival were 24.1 and 41.9 weeks, respectively. Baseline tumor biopsies from patients who responded to treatment had features of T-cell exclusion. During treatment, there was an increased T-cell infiltration, with a reduced mean distance between T cells and tumor cells. Peripheral blood immune cell composition did not significantly change during study treatment.

Conclusions Combining an intratumoral injection of CD1c (BDCA-1)$^+$ and CD141 (BDCA-3)$^+$ myDC with repeated IT administration of ipilimumab and AS01$_B$ and systemic low-dose nivolumab is safe, feasible with promising early results, worthy of further clinical investigation.

Trial registration number ClinicalTrials.gov identifier NCT03707808.

WHAT IS ALREADY KNOWN ON THIS TOPIC

⇒ Patients with advanced melanoma who progress after treatment with immune checkpoint-inhibitors and BRAF-/MEK-inhibitors (if *BRAF*^{V600} mutated) have no remaining effective treatment options. The presence of myeloid dendritic cells (myDC) in the tumor microenvironment is essential for the effectiveness of immune checkpoint blockade (ICB). The synthetic saponin-based adjuvant AS01$_B$ induces adaptive immune responses by recruiting and activating myDC.

BACKGROUND

Only a minority (25–30%) of patients with advanced melanoma treated with programmed cell death protein-1 (PD-1) and cytotoxic T-lymphocyte associated protein-4 (CTLA-4) immune checkpoint blockade (ICB) and BRAF-/MEK-targeted therapy (in case of *BRAF*^{V600} mutant melanoma) obtain

WHAT THIS STUDY ADDS

⇒ This first-in-human phase I clinical trial adds new insights regarding the therapeutic effect of intratumoral (IT) administration of the adjuvant AS01$_B$ in combination with CD1c (BDCA-1)$^+$/CD141 (BDCA-3)$^+$ myDC, plus intratumoral blockade of the cytotoxic T-lymphocyte associated protein-4 (CTLA-4) and systemic blockade of the programmed cell death protein-1 (PD-1) immune checkpoints. This first-in-human study demonstrates the feasibility and safety of this innovative approach while the durable tumor responses in 3 out of 8 study patients provide evidence for activity supporting further investigation in refractory melanoma.

HOW THIS STUDY MIGHT AFFECT RESEARCH, PRACTICE OR POLICY

⇒ This study provides evidence that the investigated combinatorial IT treatment approach offers a potential path for the induction of effector antitumor immune responses in patients with immune checkpoint inhibitor-refractory melanoma, leading to durable tumor responses even after cessation of local and systemic therapy. The combination of an immunogenic adjuvant such as AS01$_B$ with myDC is a therefore feasible and promising approach that warrants further investigation in a larger cohort. Additional translational research is needed to deepen our understanding of the (immunological) mechanisms underlying the observed tumor responses and the respective contributions of myDC, AS01$_B$ and ICB. Additionally, the present study could spark interest in continued exploration of optimized combination and timing strategies with these components to further enhance treatment outcomes. Our findings hold promise for advancing therapeutic options and potentially have significant implications for the clinical management of patients with advanced melanoma.

a durable response.[1–8] For patients with treatment-refractory melanoma, survival remains poor.[9] Therefore, an important unmet need remains for patients with melanoma that progress beyond the current standard of care.

Dendritic cells (DC) are crucial in initiating an antitumor immune response by acting as a link between the innate and adaptive immune system.[10] The population of human DC is diverse and can be divided into myeloid DC (myDC; also referred to as conventional DC (cDC)) and plasmacytoid DC (pDC).[11 12] cDC or myDC, accounting for <1% of immune cells in the peripheral blood, are characterized by the expression of CD11c and high levels of major histocompatibility complex class II molecules.[13]

Human myDC can be further divided into two major subsets based on their surface markers and functions: CD141 (BDCA-3)$^+$ or cDC1 and CD1c (BDCA-1)$^+$ or cDC2. cDC2 are more heterogeneous with a CD14+ subgroup that has been characterized as potentially immunosuppressive (also known as DC3).[14 15] Both myDC subtypes play a crucial role in initiating antigen-specific antitumor immunity by priming antitumor T-cell responses and relicensing of antitumoral T cells in the tumor microenvironment (TME). While CD141 (BDCA-3)$^+$ myDC mediate CD8$^+$ cytotoxic T-cell responses,[16–18] CD1c (BDCA-1)$^+$ myDC have been reported to mainly mediate CD4+T-cell responses and mediate immune responses induced by immunogenic cell death.[19] Their presence in the TME is crucial for initiating an antitumor immune response and for responding to ICB and adoptive T-cell therapy.[20] However, tumor growth can impede myDC recruitment to the TME, resulting in defective T lymphocyte activation and allowing metastases to escape antitumor immune responses.[21] Based on their surface markers, clinical grade immunomagnetic bead isolation of myDC has become feasible and enabled their use for clinical myDC vaccination therapy.[22]

Early-phase clinical trials have demonstrated effective immunization and tumor responses with the use of myDC-derived vaccines (based on CD1c (BDCA-1)$^+$ DC alone or in combination with pDC) in patients with advanced melanoma and prostate cancer.[23–26] The feasibility and safety of intratumoral (IT) administration of immunotherapy in solid tumors has been explored extensively.[27] Notwithstanding the sometimes impressive local tumor response rates and the approval of talimogene laherparepvec (T-VEC), a low rate of objective overall tumor response in patients with distant metastases has hampered its acceptance as a commonly used treatment modality.[28] Our research group has previously shown that IT injection of CD1c (BDCA-1)$^+$ myDC in combination with IT injection of ipilimumab and avelumab plus low-dose nivolumab (intravenous) in patients with advanced, immune checkpoint-refractory solid tumors is safe and feasible and resulted in promising antitumor efficacy.[29] Also, IT injection of the combined cell product consisting of CD1c (BDCA-1)$^+$ and CD141 (BDCA-3)$^+$ myDC in combination with the oncolytic virus T-VEC resulted in durable complete responses as well.[30]

Adjuvant system 01$_B$ (AS01$_B$) is a liposome-based adjuvant containing two immunostimulants: monophosphoryl lipid-A and QS21, a saponin isolated from the Quillaja saponaria, or soap bark tree.[31] Preclinical evidence has shown that subcutaneous co-injection of AS01$_B$ together with an antigen induces strong recruitment of cDC1 and cDC2 to the draining lymph node and antigen presentation to both CD4$^+$ and CD8$^+$ T cells in a mouse model.[32] Early findings demonstrate strong antigen-specific antibody responses in humans inducing immune cell recruitment as well as an natural killer (NK)-mediated and CD8$^+$ T-cell-mediated interferon (IFN)-γ response.[33 34] AS01$_B$ is currently a component of the commercially available recombinant vaccine Shingrix (GSK), a prophylactic vaccine preventing shingles. Its safety, when administered intramuscularly (IM), has been extensively investigated.[35] It has also been used as an adjuvant for a Wilms' tumor protein (WT1) vaccine administered IM in patients with acute myeloid leukemia and a cytomegalovirus (CMV) vaccine in patients with glioblastoma.[36 37]

In ex vivo experiments we found that AS01$_B$ was nontoxic for human myDC (unpublished results). We hypothesize that IT administration of autologous CD1c (BDCA-1)$^+$/CD141 (BDCA-3)$^+$ myDC together with

AS01$_B$ and both IT and IV immune checkpoint inhibition would have an immune-stimulatory effect triggering a more efficient antitumor immune response in patients with melanoma who do not respond to ICB. In addition, AS01$_B$ could be an attractive economical alternative for more expensive IT agents such as recombinant oncolytic viruses.

METHODS
Patients
Patients with unresectable, advanced melanoma (American Joint Committee on Cancer eighth edition stage III or stage IV), who progressed on standard-of-care therapy including PD-1 and CTLA-4 ICB and BRAF-/MEK-inhibitors (in case of $BRAF^{V600}$ mutant melanoma) were eligible. Patients needed to have at least one non-visceral lesion amenable to IT injection (either ultrasound or clinically guided). Other key inclusion criteria included age ≥18 years; Eastern Cooperative Oncology Group (ECOG) performance status of 0 or 1; normal hematological, liver, and renal function tests; and negative serological tests for HIV, syphilis, hepatitis B and C. Exclusion criteria included leptomeningeal metastases, untreated/symptomatic central nervous system metastases, systemic corticosteroid treatment, a history of autoimmune diseases, and the need for permanent therapeutic anticoagulation.

Study design and treatment
This trial is a single-arm, single dose level, phase I pilot, safety run-in cohort investigating the first-in-human IT application of AS01$_B$ in patients with pretreated melanoma at UZ Brussel. After completing screening, patients undergo leukapheresis to isolate myDC. On the day of the leukapheresis (day 1), a biopsy of the lesion chosen for IT treatment is performed. Afterwards (on the same day), 10 mg of ipilimumab is injected into one or several accessible (either clinical or ultrasound guided) lesions and patients receive an IV administration of nivolumab 10 mg. Twenty-four hours later, all myDC (suspension volume based on lesion size) are injected into the same lesion(s) together with 50 µg (0.5 mL) AS01$_B$. Patients continue to receive IT administration of ipilimumab (10 mg) and AS01$_B$ (50 µg) as well as intravenous administration of nivolumab 10 mg every 2 weeks thereafter until planned end of study treatment (week 51) after which all study treatment is discontinued. On disappearance of a previously injected lesion, IT injection of ipilimumab and AS01$_B$ was performed into another lesion after patient re-evaluation when feasible and safe. Full study protocol can be found in online supplemental file 3.

Leukapheresis and isolation of myDC
Peripheral blood mononuclear cells were obtained by leukapheresis of 15 L of blood using the Cobe Spectra device (Terumo Europe, Leuven, Belgium). First, CD14$^+$ and CD19$^+$ cells were depleted with the CliniMACS CD14 and CD19 reagents followed by a positive selection of CD1c (BDCA-1)$^+$ myDC and CD141 (BDCA-3)$^+$ myDC by using CliniMACS CD1c (BDCA-1)-biotin microbeads, CliniMACS CD141 (BDCA-3)-biotin microbeads and CliniMACS Anti-Biotin Reagent (Miltenyi) using the CliniMACS Prodigy platform (Miltenyi Biotec, Bergisch Gladbach, Germany). The isolated CD1c (BDCA-1)$^+$ and CD141 (BDCA-3)$^+$ myDC fraction was concentrated by centrifugation and resuspended in phosphate-buffered saline/EDTA (Miltenyi) containing 0.5% human albumin to obtain a cell suspension at volume desired for clinical administration (according to tumor diameter, up to maximum 4 mL). The characterization of the myDC product is described in the supplementary methods (in online supplemental materials) and was performed on the final cell product (after volume reduction).

Assessment of tumor response and toxicity
Tumor assessment was performed by whole-body fluorodeoxyglucose (^{18}F) FDG positron emission tomography-CT ([^{18}F] FDG-PET/CT) at baseline and every 12 weeks thereafter. Objective response rates were evaluated using the modified Response Evaluation Criteria in Solid Tumors for immunotherapy (iRECIST V.1.1).

Safety was assessed continuously. Clinical as well as hematological and biochemical parameters were assessed before every administration of study medication. Adverse events (AE) were classified for type, frequency, and severity according to the National Cancer Institute Common Terminology Criteria for Adverse Events (V.5.0).

Determination of lymphocyte subsets in peripheral blood
See supplementary methods (in online supplemental materials).

Tumor biopsies and immunohistochemistry
When feasible and safe, a tru-cut biopsy was performed at baseline (day 1), day 3, and at every IT administration thereafter (every 2 weeks). Routine immunohistochemistry (IHC) stainings for SOX10 (clone SP267), PD-L1 (clone 22C3), and CD8 (SP57) were performed for diagnostic reasons and to select relevant biopsies for further multiplex immunohistochemistry (mIHC) analysis.

Multiplex immunohistochemistry staining
See supplementary methods (in online supplemental materials).

mIHC acquisition and quantification
The mIHC slides were imaged using the PhenoImager HT scanner (Akoya Biosciences). Whole-slides were scanned with all five standard epi-fluorescence filters (DAPI, FITC, Cy3, Texas Red and Cy5) at 20× magnification using appropriate exposure times. The whole tissues were then selected for multispectral imaging at 20× magnification. To allow for unmixing of the multispectral images (MSI), a spectral library was built from pure emission spectrum of each Opal fluorophore and DAPI obtained by single pan-cytokeratin staining on formalin-fixed paraffin-embedded (FFPE) tonsil sections.

The autofluorescence spectrum was generated from an unstained FFPE melanoma lymph node metastasis section. The MSI were unmixed using the spectral library and the tissue autofluorescence was removed followed by digital quantification (tissue and cell segmentation and cell phenotyping) in inForm Tissue Analysis Software (V.2.6.0, Akoya Biosciences).

Development of quantification algorithms: See supplementary methods (in online supplemental materials).

The inForm data were analyzed in RStudio IDE using the phenoptrReports packages (V.0.3.2 developed by Kent S Johnson, Akoya Biosciences) to quantify the number of B cells (exclusively positive for CD20), CD4$^+$ T cells (exclusively positive for CD4), CD8$^+$ T cells (exclusively positive for CD8), regulatory T cells (exclusively positive for CD4 and FOXP3), macrophages (exclusively positive for CD68 and positive or negative for SOX10) and tumor cells (exclusively positive for SOX10) in both tumor and peritumoral area. Additionally, (peri)tumoral areas (mm^2) and nearest neighbor distances (µm) between tumor cells and CD4$^+$/CD8$^+$ T cells have been quantified using the same R phenoptrReports package. For each biopsy, the quantifications mentioned above have been performed on MSI selected by pathologists as representative for tumor or peritumoral regions, excluding any healthy or necrotic tissue regions.

Statistical analysis

Descriptive statistics are provided for baseline demographics, treatment disposition, and safety. Statistical tests used to assess significance are indicated in the figure legends. Non-parametric Mann-Whitney test was employed for data defined by two groups (n=3) and corrected for multiple testing using the Holm-Sidak method where necessary. For survival analysis (progression-free survival (PFS) and overall survival (OS)), a Kaplan-Meier estimate was applied. Statistical analysis was performed in SPSS V.28 and GraphPad Prism V.10.0.2. Graphical representations were made with GraphPad Prism V.10.0.2 and BioRender.

Patients were deemed evaluable for response when they reached their first on-treatment evaluation. The database was locked on July 11, 2023.

RESULTS
Patient characteristics

Between July 2021 and May 2022, eight female patients were recruited. The Consolidated Standards of Reporting Trials diagram is provided in figure 1. The median age was 64 years (range 33–83). Four patients presented with stage IV—M1a disease and four patients with stage IV—M1c disease. Six patients had ECOG=0, two patients had ECOG=1. All patients had been pretreated with both anti-PD-1 and anti-CTLA-4 monoclonal antibodies, either as a sequential mono or combination therapy. An *NRAS*^{Q61} mutation was documented in the melanoma of four patients, an *SMARC* mutation in two patients, a
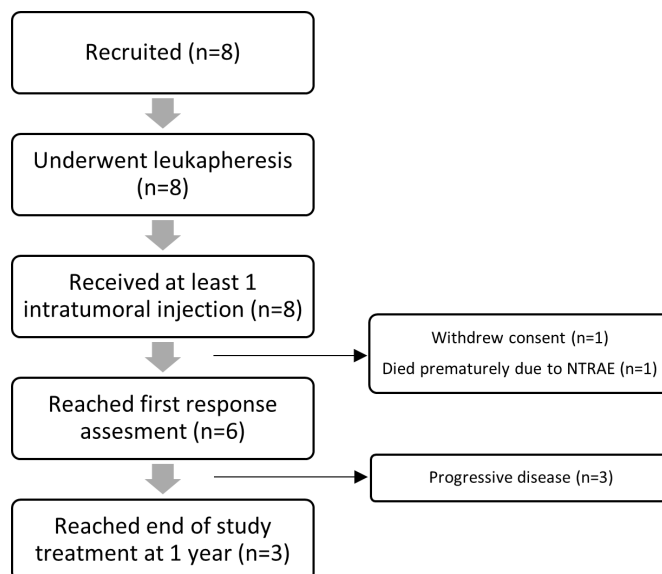

Figure 1 Disposition of patients enrolled in the trial (Consolidated Standards of Reporting Trials diagram). NTRAE, not treatment-related adverse event.

GNAQ^{T96S} mutation in one patient, and an *MEK1*$^{K57\_G61del}$ mutation also in one patient. Baseline characteristics are summarized in table 1 and the prior lines of treatment for each individual patient are listed in online supplemental figure 1.

Isolation and characterization of myDC

Isolation of myDC was successful in all patients and no unexpected or serious AEs occurred. Median number of isolated myDC was 20.7×10^6 (range 14.8–34.9). Median viability of the isolated cell product was 86.5%, the median number of CD1c (BDCA-1)$^+$ DC injected was 19.34×10^6, the median number of CD141 (BDCA-3)$^+$ DC injected was 1.85×10^6. Full cell counts on an individual patient basis can be found in online supplemental table 2. The median composition of the myDC product contained 3.49% CD141 (BDCA-3)$^+$ myDC, 53.5% CD1c (BDCA-1)$^+$ myDC and 1.85% pDC (online supplemental figure 2A and D). The composition of the autologous cell product was comparable between responders and non-responders. The myDC had an immature phenotype with low CD40, CD80, CD83 and CD274 expression and high CD86 and HLA-ABC expression (online supplemental figure 2B). A higher percentage of CD141 (BDCA-3)$^+$ myDC were CD80 positive and had a higher expression level of HLA-ABC, indicative of a slightly more mature cell state compared with the CD1c (BDCA-1)$^+$ myDC (online supplemental figure 2B, C). The phenotype of the myDC product did not differ significantly between responders and non-responders, except for a lower percentage of CD86$^+$ cells in the CD1c (BDCA-1)$^+$ myDC in responders versus non-responders (p=0.0174).

Treatment disposition

All patients received at least one IT and one intravenous treatment. The median number of intravenous treatments

Table 1 Baseline characteristics

	Patients, n (%)
Median age (years)	64 (range 33–83)
Gender	
Male	0
Female	8 (100)
ECOG performance status	
0	6 (75)
1	2 (25)
Disease stage	
IV-M1a	4 (50)
IV-M1c	4 (50)
Prior types of therapy	
Anti-PD-1	8 (100)
Anti-CTLA-4	8 (100)
Chemotherapy	2 (25)
Imiquimod (topical)	1 (12.5)
Trametinib+low dose dabrafenib[43]	2 (25)
Median prior lines of therapy	2 (range 2–5)
Molecular analysis	
$NRAS^{Q61}$	4 (50)
SMARC	2 (25)
$MEK1^{K57\_G61del}$	1 (12.5)
$GNAQ^{T96S}$	1 (12.5)

CTLA-4, cytotoxic T-lymphocyte associated protein-4; PD-1, programmed cell death protein-1.

was 8.5 (range 1–24), and the median number of IT treatments was 4.5 (range 1–12). In all but two patients, a single metastasis was injected. In patient 5, initially several small subcutaneous in transit metastases were injected. Following complete regression of these metastases, subsequently an axillary lymph node was injected. In patient 7, three different metastases were consecutively injected following the complete regression of an individual metastasis. Three patients (patient 4, 7 and 8) were electively switched to standard dosing of nivolumab 480 mg every 4 weeks after the complete regression of the metastases treated by IT (respectively, after 40, 49 and 24 weeks of study treatment). Three patients (patient 4, 7 and 8) reached the planned end of study treatment (week 51) without signs of progression and have ended both their IT and systemic therapy while remaining in follow-up. Graphical representations of the treatment disposition of all patients (except for patient 7 which is discussed later in more detail) can be found in online supplemental figure 3.

Safety and adverse events
The most frequent AEs were local injection site reactions (63%) and fatigue (63%). These AEs were mild (grade 1 or 2) and self-limiting without requiring any medical intervention or discontinuation of the study treatment schedule. The clinical inflammatory responses observed at the injection site varied among patients: some experienced local injection site reactions such as tenderness and redness that lasted for 3–5 days, while others did not have any noticeable reaction. One patient (patient 2) died due to a treatment-unrelated grade 5 AE while on treatment (brain hemorrhage due to rupture of an arteriovenous malformation). No patients required corticosteroid treatment to recover from an immune-related AE. Treatment was temporarily discontinued once in three patients, due to fatigue (n=1), diverticulitis (n=1) and stomach pain (n=1). All patients resumed study treatment at the next visit without a need for additional medical intervention. One patient experienced an episode of fever (grade 1) following the first injection of myDC and $AS01_B$ on day 2 of the study treatment. The most frequent AEs are summarized in table 2, a complete list can be found in online supplemental table 3.

Clinical outcome
Of the eight included patients, six patients were evaluable for tumor response. One patient withdrew consent after one treatment cycle (patient 1), and one patient suffered a grade 5 treatment-unrelated AE before the first response evaluation (patient 2). Among the six evaluable patients,

Table 2 Adverse events with incidence >1 or grade ≥3 according to Common Terminology Criteria for Adverse Events V.5.0; n (%)

	Grade 1	Grade 2	Grade 3	Grade 4	Grade 5
Arthralgia	2 (25)	0	0	0	0
Dyspepsia	2 (25)	0	0	0	0
Fatigue	5 (63)	2 (25)	0	0	0
Injection site reaction	5 (63)	0	0	0	0
Intracranial hemorrhage	0	0	0	0	1 (13)
Muscle cramp	3 (38)	0	0	0	0
Lymphocyte count decreased	0	0	1 (13)	0	0
Nausea	2 (25)	0	0	0	0
Pain	2 (25)	3 (38)	0	0	0

two patients (25%) obtained a complete response (CR), one patient (12.5%) obtained a partial response (PR), one patient (12.5%) had stable disease (SD), and two patients (25%) had progressive disease (PD) according to iRECIST 1.1 criteria (figure 2A). The disease control rate (CR+PR+SD) was 50%. Median duration of response was not reached. Four patients (50%) had complete regression of their injected lesion(s), with a confirmed pathological CR of the injected metastases in three patients.

At database lock, three patients were alive and progression free; five patients had died (melanoma progression was the cause of death in four of them). Median PFS was 24 weeks (range 2–75 weeks), median OS was 42 weeks (range 5–75 weeks) (figure 2B). CRs were durable, with two patients remaining disease free more than 1 year since start of study treatment while no longer receiving any treatment. Clinical outcome and response kinetics of evaluable patients are summarized in figure 2A. Individual patient characteristics and outcome can be found in online supplemental table 4 and online supplemental figure 3.

Patient 7, illustrated in figure 3A, experienced progressive tumor reduction over the course of several months: three different lesions (inguinal lymph node lesion and two distinct subcutaneous lesions in the leg) were sequentially injected and all responded to therapy. Moreover, a clear response was observed in several non-injected lesions (lung, soft tissue). After 24 weeks they obtained a PR that is currently ongoing for more than 12 months since the start of treatment with further progressive reductions in disease burden. Patient 5 presented with bone, subcutaneous and axillary lymph node lesions. On injection of the subcutaneous lesions, a CR of the injected lesions was observed. However, subsequent injection of the axillary lymph node lesion did not yield a response and the subcutaneous nodules at the elbow reappeared over the course of 3 months. On re-injection, these did not respond, and the patient continued to progress.

Effect of treatment on immune composition in the blood
At each treatment cycle, the immune blood cell composition was analyzed. At baseline, we did not observe significant differences between the levels of neutrophils, basophils, eosinophils, lymphocytes, monocytes (online supplemental figure 4A), and neutrophil-to-lymphocyte ratio (online supplemental figure 4B) in responders (PR/CR as best objective response (BOR)) versus non-responders (PD as BOR) and the patient with SD (patient 5). Furthermore, flow cytometric analysis to identify total T cells ($CD3^+$), $CD4^+$ T cells, $CD8^+$ T cells, regulatory T cells (Tregs) ($CD4^+CD25^{hi}$), B cells ($CD19^+$), and NK cells ($CD56^+/CD16^+$) did not show significant differences in the frequencies of the identified cell types at baselines between responders and non-responders (online supplemental figure 4C–E).

Subsequently, we investigated whether the composition of the immune infiltrate in the blood changed on treatment. To this end, we calculated the median of all on-treatment values for each patient and compared this with the baseline values. We did not observe significant differences between baseline and on-treatment values for any of the cell types, neither when considering all patients nor when grouping patients based on their clinical response (responders and non-responders/SD) (online supplemental figure 5A). Furthermore, we expanded these analyses to look into naïve, stem cell memory cells, terminally differentiated effector cell, central memory and effector memory T cells (online supplemental figure 5B) as well as in the evolution of myDC subtypes in the peripheral blood (online supplemental figure 5C). We observed a limited but significant (p=0.02) increase in CD4+central memory T (T_{CM}) cells in the non-responders. None of the other cell populations showed significant changes from baseline while on treatment, nor was there any correlation with response.

Immune composition of tumor and peritumoral regions in baseline and on-treatment biopsies
Patients 1 and 8 were omitted from this analysis since no relevant or insufficient material was available for mIHC analysis. For quantitative mIHC analysis, patients were divided in two groups based on their clinical response: responders (patients 3 and 6) and non-responders (patients with 4 and 7). Patients 2 and 5 are discussed separately. Tissue segmentation, based on SOX10 staining, allowed to distinguish tumor and peritumoral areas in the biopsies. Immune cell composition was assessed in both regions separately. The proportion of tumor area within the evaluated tissue slide is represented for each biopsy in figure 4A,B (upper panel).

Non-responders showed a total absence (patient 6) or minor IT immune influx (patient 3), both at baseline and throughout treatment (figure 4A, middle panel). In contrast to the IT region, a substantial immune influx (34.11%±7.65) was observed at baseline in the peritumoral region of non-responders and was dominated by macrophages, $CD4^+$ T cells and $CD8^+$ T cells (figure 4A, lower panel). These results are suggestive of the phenomenon known as T-cell exclusion, where T cells are restricted to the tumor periphery. Figure 4C depicts a microscopic image of patient 3 biopsy at baseline and on-treatment (week 2), illustrating exclusion of both $CD4^+$ and $CD8^+$ T cells from the $SOX10^+$ tumor region.

In the responders, we generally observed T-cell excluded tumor regions at baseline with T-cell presence being limited to the peritumoral regions (figure 4B). In contrast to the non-responders, a pronounced increase of T cells was observed in the peritumoral region of responders on treatment (18.69%±1.76) in comparison to baseline (9.75%±1.98). In patient 7 (figure 3B) this peritumoral T-cell influx on treatment was also reflected in the tumor region which showed a noticeable T-cell fraction (dominated by $CD8^+$ T cells) in both lesions. In patient 4, the limited tumor area in the on-treatment tissue sections analyzed by mIHC did not allow in-depth investigation of the immune cell composition in the tumor region.
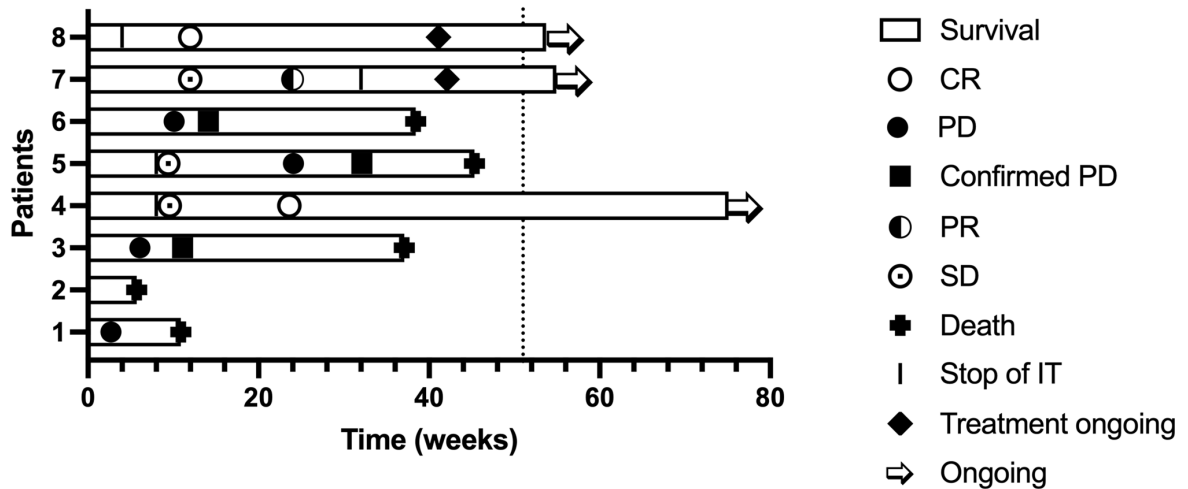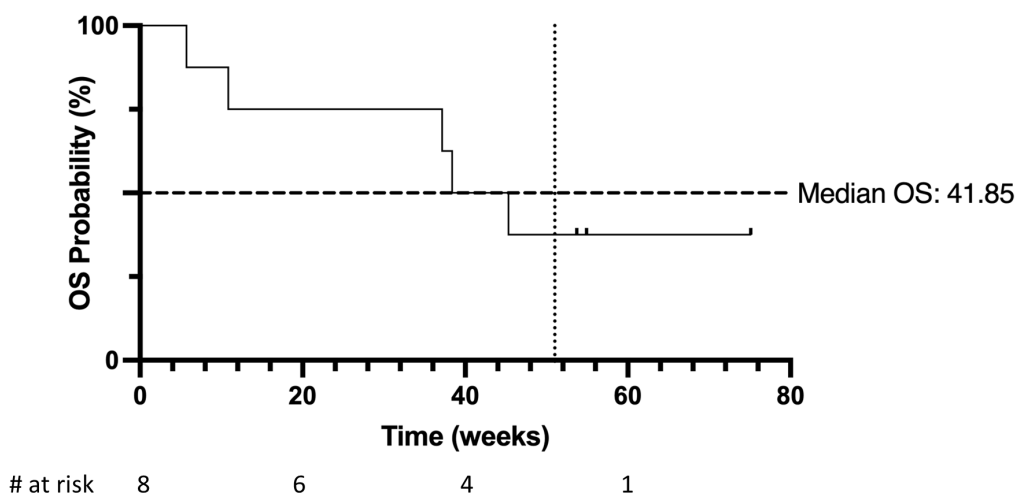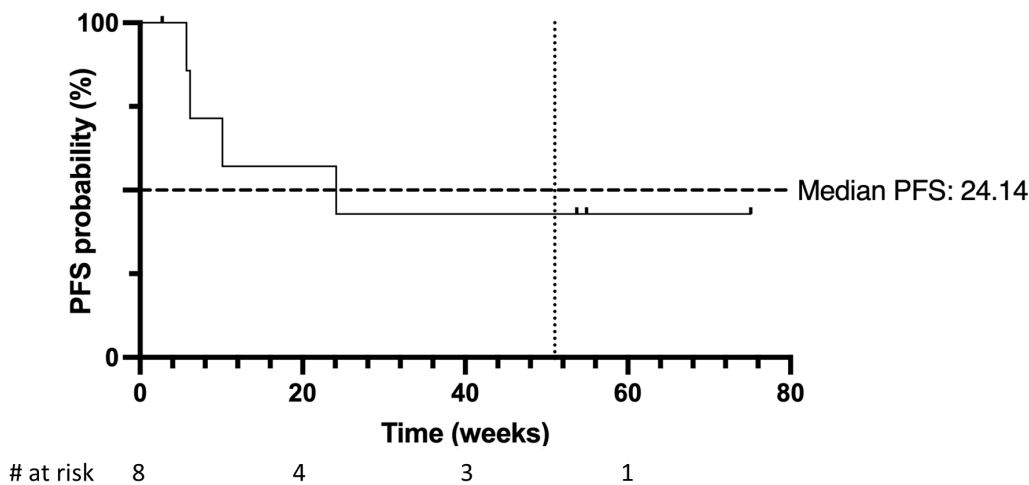
Figure 2 (A) Swimmer plot representing response at each evaluation, duration of treatment and survival of each patient at data cut-off. Bars depict overall survival. Arrow indicates patient remaining alive. Complete response (CR), progressive disease (PD), partial response (PR), stable disease (SD) marked as per figure legend. Stop of intratumoral indicates end of intratumoral injections (continuation of intravenous treatment). Planned end of study treatment protocol (52 weeks) is depicted as vertical dotted line. (B) Kaplan-Meier survival estimates for progression-free survival (PFS) (left) and overall survival (OS) (right) in weeks since start of study treatment. Median survival in weeks is indicated on the curve as a horizontal dotted line. Planned end of study treatment protocol (52 weeks) is depicted as vertical dotted line.
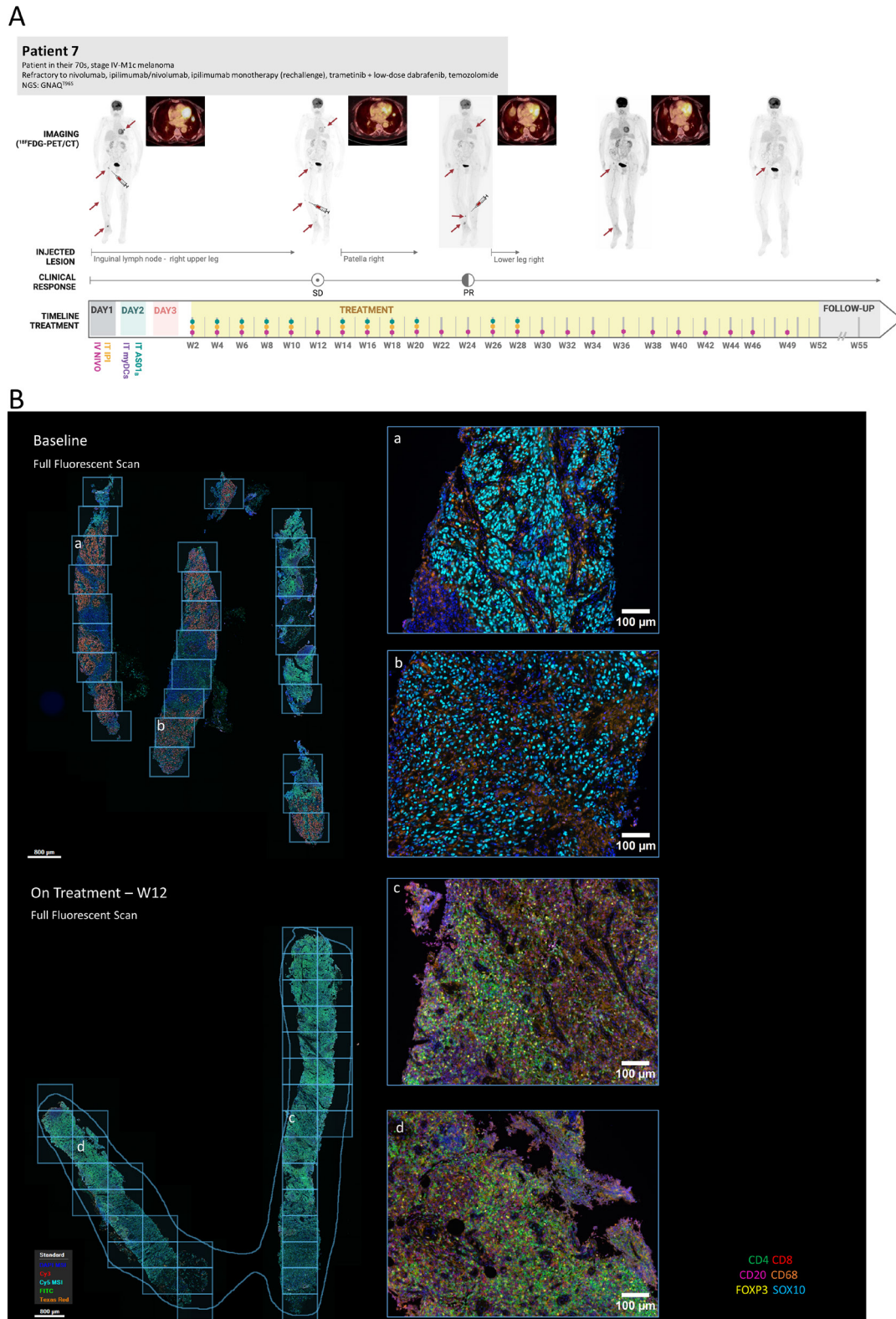
Figure 3 Case illustration and treatment disposition of patient 7. (A) Timeline depicts time since first treatment administration. Dots indicate treatment administration as indicated on day 1 and day 2. Arrows indicate significant lesions. Syringe indicates injected lesion. Whole body 18F-FDG-PET/CT images are shown, together with a zoomed axial fusion image (PET/CT) of the lung lesion (non-injected). (B) Representative images from multiplex immunohistochemistry analysis at baseline (upper panel) and while on treatment (week 12, lower panel). Left images are overview full fluorescent scans before spectral deconvolution with indication (grid) of individual multispectral images (MSI) analyzed. Right images show selected MSI and analysis of immune cell composition of tumor region indicating a progressive decrease of detectable tumor region and influx of immune cells (mostly CD4 and CD8) while on treatment. IV, intravenous; IT, intratumoral; myDCs, myeloid dendritic cells; NGS, next generation sequencing results (mutated genes); PD, progressive disease; PR, partial response; SD, stable disease.
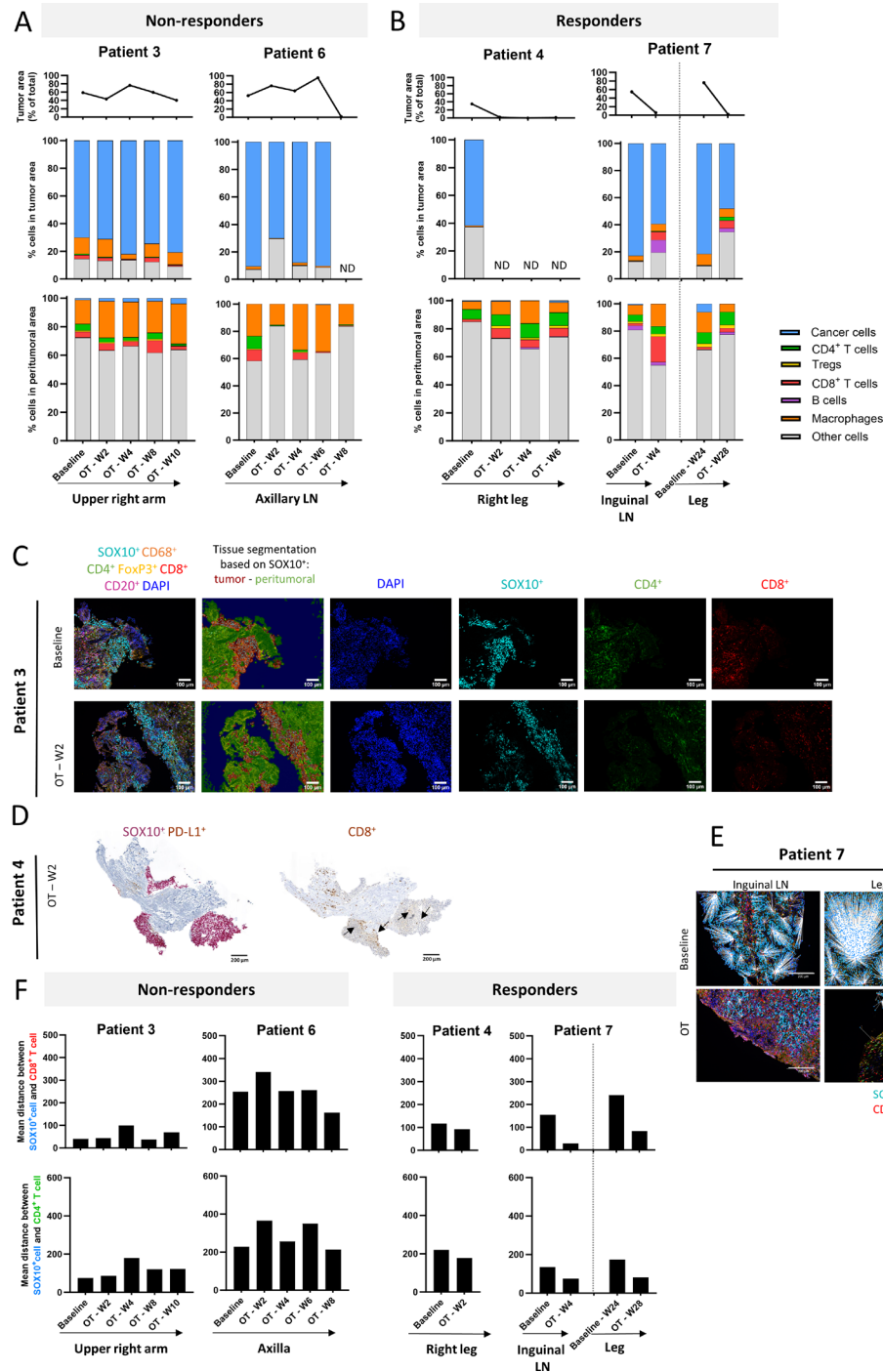
Figure 4 Immune composition of tumor and peritumoral regions: Results from multiplex immunohistochemistry analysis. (A and B) Upper panel: proportion of tumor cells (SOX10$^+$) in biopsy sample. Middle panel depicts cellular composition of the tumor area. Lower panel depicts cellular composition of the peritumoral area. Time on treatment and injected lesion is indicated beneath the graphs. For patient 7, first biopsy (at 24 weeks on treatment) of leg lesion before intratumoral injection of this lesion was considered as baseline for this lesion. (C) Microscopic multiplex immunohistochemistry image of patient 3 tumor samples at baseline and on-treatment (week 2), illustrating exclusion of both CD4$^+$ and CD8$^+$ T cells from the SOX10$^+$ tumor region. Scale bar=100 µm. DAPI, 4',6-diamidino-2-fenylindool; FoxP3, forkheadbox P3. (D) Immunohistochemistry slide showing SOX10 and CD8 immunohistochemistry staining on consecutive slides (containing a considerable tumor area) demonstrating presence of CD8$^+$ T cells in the tumor region. Scale bar=200 µm. (E) Visual representation of decreasing distance between CD8+T cells and SOX10+ melanoma cells in patient 7, both baseline and on-treatment. For patient 7, first biopsy (at 24 weeks on treatment) of leg lesion before intratumoral injection of this lesion was considered as baseline for this lesion. White lines indicate distance between respective cells. Scale bar=200 µm. (F) Graphs representing mean distance between SOX10$^+$ melanoma cells and CD8+ (upper panel) or CD4+ (lower panel) T cells in non-responders (left) and responders (right) as measured on one tissue slide. A notable decrease can be observed in both CD4+and CD8+ T cells in the responding patients. Tregs = regulatory T cells, ND = not detected, LN = lymph node

Nevertheless, SOX10 and CD8 IHC staining on consecutive slides (containing a considerable tumor area) showed presence of CD8$^+$ T cells in the tumor region (figure 4D), suggesting an influx of T cells in the tumor area on treatment at week 2. Concurrently, the mean distance between SOX10$^+$ melanoma cells and nearest CD8$^+$ T cells as well as nearest CD4$^+$ T cells notably decreased in responder patients on treatment as compared with baseline (figure 4E,F) whereas this phenomenon was not observed in the non-responders (figure 4F). No trends were observed in the distance between melanoma cells and other immune cell types.

On investigating the immune composition of patient 2 in the (peri)tumoral area at baseline and on-treatment, we observed trends similar to our observations in responders: treatment induced an influx of T cells in the peritumoral area (6.72%±1.40) which was also reflected in the tumor area (2.58%±0.49), mainly as a small CD8$^+$ T-cell fraction (online supplemental figure 6A). This treatment-induced T-cell influx is remarkable given that the patient started with an immune infiltrate that almost exclusively consisted of macrophages at baseline in both the tumor (13.05%, whereof 12.91% macrophages) and peritumoral (21.72%, whereof 20.67% macrophages) area. We also observed a decrease in distance between melanoma cells and both nearest CD8$^+$ and CD4$^+$ T cells on treatment in comparison to baseline (online supplemental figure 6B, C).

Finally, an on-treatment biopsy of an elbow lesion of patient 5, who had different responses in subsequently injected lesions (CR in subcutaneous elbow lesions vs PD in axillary lymph node lesion), was suggestive for the phenomena of T-cell exclusion with majority of both CD4$^+$ and CD8$^+$ T cells being restricted to the peritumoral area (online supplemental figure 6A–D). Unfortunately, no baseline biopsies of both the elbow and axillary lesions were available. On treatment of the elbow lesion, the T-cell infiltration was increasing in the tumor area as well and potentially could be related to the pathological complete response (pCR) that was eventually observed in this lesion. In contrast, in the axillary lesion, the presence of T cells remained restricted to the peritumoral area and barely reached the tumor area. Tregs numerously emerged in the peritumoral region of both the elbow and axilla lesions.

Several patients (2, 3, 5 and 7) showed a substantial macrophage fraction in the tumor area both at baseline and throughout treatment. Zooming in on this fraction, we found that part of these macrophages stained double positive for CD68 and SOX10. Interestingly, for patients 2 and 7 (non-lymph node (LN) lesions) these SOX10$^+$CD68$^+$ cells represent the majority of the macrophage population in the tumor area (66.02%±8.26) (online supplemental figure 6E).

DISCUSSION

In this phase I clinical trial, we investigated if it was possible to (re)invigorate cancer immunity by IT administration of CD1c (BDCA-1)$^+$ and CD141 (BDCA-3)$^+$ myDC, ICB and the saponin-based adjuvant AS01$_B$ in patients with advanced treatment refractory melanoma, combined with IT CTLA-4 and systemic PD-1 blockade. This investigation builds further on our previously reported results with intertumoral injection of autologous CD1c (BDCA-1)$^+$ and CD141 (BDCA-3)$^+$ myDC with ICB or T-VEC.[29 30]

In eight patients, we demonstrated acceptable safety of this combinatorial immunotherapy, with mainly low-grade treatment-related AEs. Administration of myDC was well-tolerated, with only one patient experiencing G1 fever following the first administration of myDC and AS01$_B$. The repeated IT administration of AS01$_B$ (: first-in-man investigation) neither resulted in unexpected safety signals. This suggests that the immunostimulant effect of AS01$_B$ is heterogeneous between patients and wears off relatively fast, as has been observed in preclinical models.[32] Previously, administration of an AS01$_B$ adjuvanted vaccine was shown to induce rapid and transient increases in serum levels of several cytokines including interleukin-6 and IFN-γ. Levels of all cytokines decreased rapidly with return to baseline by day 7.[38] This might provide a potential explanation for the observed AEs, including transient fever and fatigue, in our study. Whether an ongoing inflammatory response would be beneficial for a sustained antitumoral effect is unknown. However, if ongoing inflammation needs to be achieved to induce a stronger antitumor response, a higher dose or more frequent administration of AS01$_B$ could be explored. Recently, an important effect of saponin-based adjuvants with cDC2 was reported, leading to increased cross-presentation of antigens.[39] Such observations point to an essential role for the CD14$^+$ (CD5$^-$ CD163$^+$) cDC2 subset (also known as DC3) which is not included in our myDC cell product in light of their possible "immunosuppressive nature" as described previously.[14] Further research is needed to investigate the precise effect of AS01$_B$ on the individual DC subtypes present in our autologous therapeutic cell product.

Promising early evidence for antitumor activity was observed in our phase I trial with a disease control rate of 50% and three durable responses in patients refractory to ICB (including anti-PD-1 and anti-CTLA-4). Considering that two patients did not complete their first response evaluation and may not have been exposed to study treatment for a sufficient duration, four out of the other six patients (66.6%) achieved disease control, with two CRs, one PR, and one SD. The observed responses were durable (>1 year and ongoing) and were maintained after stopping all therapy indicating that an effective and lasting immunological response had been achieved. Responses in injected lesions matched or exceeded the best overall response, aligning with similar findings reported from a large cohort of patients treated with IT immunotherapy.[40] While patient 2 could not be evaluated for response, mIHC analysis on early on-treatment biopsies revealed evidence of an immune response in this patient. Overall, while the results of this study should be

interpreted with caution due to the limited sample size and the context of a selected patient population but provide first evidence supportive of a conceptual proof of concept and deserving further clinical investigation.

The use of an IT approach for treatment administration provided a unique opportunity to perform serial biopsies of the injected lesions to investigate the presence of tumor cells and to document treatment-induced changes in the immunological infiltrate in these injected lesions using mIHC. We observed baseline phenotypes of T-cell excluded tumors, with an influx of T cells in the patients that are responding to therapy as well as a decrease in mean distance between T cells and tumor cells. Precaution should be taken for lesions located in a lymph node, due to possible skewing of mIHC results because of the natural presence of immune cells (eg, B cells were only observed in lymph node lesions).

Of note, on mIHC we observed an important fraction of SOX10+CD68+ macrophages within the macrophage population in the tumor region, which was more pronounced in responders (patients 2 and 7) compared with non-responders (patients 3 and 5). Possibly, these SOX10+CD68+ cells are macrophages that have acquired tumor cell material through phagocytosis or trogocytosis.[41] However, we cannot exclude that these are CD68+ macrophages in close contact to SOX10+ tumor cells. Alternatively, expression of SOX10 has been described in single-cell sequencing experiments in glioma as high in M1 macrophages.[42] While we do not have enough tissue material today, it would be interesting to further characterize these macrophages in future trials.

The promising early activity and tolerability observed in this phase I trial warrant further investigation in larger cohorts and potentially in phase II or III trials. Fine-tuning the dose and schedule of $AS01_B$ administration may be explored to maximize its immunostimulatory effect. Additionally, in vitro studies as well as further translational research on tumor tissue can help elucidate the mechanism of action of $AS01_B$ and its interaction with myDC and the TME.

CONCLUSIONS

In conclusion, IT administration of autologous CD1c (BDCA-1)$^+$/CD141 (BDCA-3)$^+$ myDC plus ipilimumab and $AS01_B$ in combination with intravenous low-dose nivolumab in patients with immune checkpoint-refractory advanced melanoma has shown to be feasible and safe, with no unexpected safety signals. We have observed encouraging early signs of clinical activity in 50% of patients with a sustained CR in 25%. In tumor biopsies from responding patients, we observed T-cell exclusion at baseline, while on treatment the tumor became infiltrated with T cells, resulting in a decreased mean distance between tumor cells and T cells. Given these observations, the treatment concept deserves further clinical evaluation.

Author affiliations
[1]Department of Medical Oncology/Laboratory for Medical and Molecular Oncology (LMMO), Vrije Universiteit Brussel (VUB)/Universitair Ziekenhuis Brussel (UZ Brussel), Brussels, Belgium
[2]Molecular Immunology Unit (MIU), Institut Jules Bordet, Université Libre de Bruxelles, Brussels, Belgium
[3]Department of Radiology, Vrije Universiteit Brussel (VUB)/Universitair Ziekenhuis Brussel (UZ Brussel), Brussels, Belgium
[4]Department of Pathology, Vrije Universiteit Brussel (VUB)/Universitair Ziekenhuis Brussel (UZ Brussel), Brussels, Belgium
[5]Department of Hematology, Stem Cell Laboratory, Vrije Universiteit Brussel (VUB)/ Universitair Ziekenhuis Brussel (UZ Brussel), Brussels, Belgium

ORCID iDs
Jens Tijtgat http://orcid.org/0000-0003-1688-8940
Julia Katharina Schwarze http://orcid.org/0000-0001-8990-5380
Sandra Tuyaerts http://orcid.org/0000-0003-1255-8071
Bart Neyns http://orcid.org/0000-0003-0658-5903

REFERENCES
1 Wolchok JD, Chiarion-Sileni V, Gonzalez R, et al. Overall survival with combined nivolumab and ipilimumab in advanced melanoma. *N Engl J Med* 2017;377:1345–56.

2 Robert C, Schachter J, Long GV, *et al*. Pembrolizumab versus ipilimumab in advanced melanoma. *N Engl J Med* 2015;372:2521–32.

3 Postow MA, Chesney J, Pavlick AC, *et al*. Nivolumab and ipilimumab versus ipilimumab in untreated melanoma. *N Engl J Med* 2015;372:2006–17.

4 Larkin J, Chiarion-Sileni V, Gonzalez R, *et al*. Combined nivolumab and ipilimumab or monotherapy in untreated melanoma. *N Engl J Med* 2015;373:23–34.

5 Hodi FS, O'Day SJ, McDermott DF, *et al*. Improved survival with ipilimumab in patients with metastatic melanoma. *N Engl J Med* 2010;363:711–23.

6 Robert C, Karaszewska B, Schachter J, *et al*. Improved overall survival in melanoma with combined dabrafenib and trametinib. *N Engl J Med* 2015;372:30–9.

7 Larkin J, Chiarion-Sileni V, Gonzalez R, *et al*. Five-year survival with combined nivolumab and ipilimumab in advanced melanoma. *N Engl J Med* 2019;381:1535–46.

8 Tawbi HA, Schadendorf D, Lipson EJ, *et al*. Relatlimab and nivolumab versus nivolumab in untreated advanced melanoma. *N Engl J Med* 2022;386:24–34.

9 Switzer B, Puzanov I, Skitzki JJ, *et al*. Managing metastatic melanoma in 2022: a clinical review. *JCO Oncol Pract* 2022;18:335–51.

10 Steinman RM. Decisions about dendritic cells: past, present, and future. *Annu Rev Immunol* 2012;30:1–22.

11 Villani A-C, Satija R, Reynolds G, *et al*. Single-cell RNA-seq reveals new types of human blood dendritic cells, monocytes, and progenitors. *Science* 2017;356.

12 Wculek SK, Cueto FJ, Mujal AM, *et al*. Dendritic cells in cancer immunology and immunotherapy. *Nat Rev Immunol* 2020;20:7–24.

13 Sakref C, Bendriss-Vermare N, Valladeau-Guilemond J. *Phenotypes and functions of human dendritic cell subsets in the tumor microenvironment*. Springer US, 2023: 17–35.

14 Bakdash G, Buschow SI, Gorris MAJ, *et al*. Expansion of a BDCA1+CD14+ myeloid cell population in melanoma patients may attenuate the efficacy of dendritic cell vaccines. *Cancer Res* 2016;76:4332–46.

15 Richter L, Landsverk OJB, Atlasy N, *et al*. Transcriptional profiling reveals monocyte-related macrophages phenotypically resembling DC in human intestine. *Mucosal Immunol* 2018;11:1512–23.

16 Liu J, Rozeman EA, O'Donnell JS, *et al*. Batf3(+) DCs and type I IFN are critical for the efficacy of neoadjuvant cancer immunotherapy. *Oncoimmunology* 2019;8:e1546068.

17 Spranger S, Dai D, Horton B, *et al*. Tumor-residing Batf3 dendritic cells are required for effector T cell trafficking and adoptive T cell therapy. *Cancer Cell* 2017;31:711–23.

18 Broz ML, Binnewies M, Boldajipour B, *et al*. Dissecting the tumor myeloid compartment reveals rare activating antigen-presenting cells critical for T cell immunity. *Cancer Cell* 2014;26:638–52.

19 Di Blasio S, Wortel IMN, van Bladel DAG, *et al*. Human CD1c(+) DCs are critical cellular mediators of immune responses induced by immunogenic cell death. *Oncoimmunology* 2016;5:e1192739.

20 Pittet MJ, Di Pilato M, Garris C, *et al*. Dendritic cells as shepherds of T cell immunity in cancer. *Immunity* 2023;56:2218–30.

21 Salmon H, Idoyaga J, Rahman A, *et al*. Expansion and activation of CD103(+) dendritic cell progenitors at the tumor site enhances tumor responses to therapeutic PD-L1 and BRAF inhibition. *Immunity* 2016;44:924–38.

22 Bol KF, Schreibelt G, Rabold K, *et al*. The clinical application of cancer immunotherapy based on naturally circulating dendritic cells. *J Immunother Cancer* 2019;7:109.

23 Westdorp H, Creemers JHA, van Oort IM, *et al*. Blood-derived dendritic cell vaccinations induce immune responses that correlate with clinical outcome in patients with chemo-naive castration-resistant prostate cancer. *J Immunother Cancer* 2019;7:302.

24 Schreibelt G, Bol KF, Westdorp H, *et al*. Effective clinical responses in metastatic melanoma patients after vaccination with primary myeloid dendritic cells. *Clin Cancer Res* 2016;22:2155–66.

25 Prue RL, Vari F, Radford KJ, *et al*. A phase I clinical trial of CD1c (BDCA-1)+ dendritic cells pulsed with HLA-A*0201 peptides for immunotherapy of metastatic hormone refractory prostate cancer. *J Immunother* 2015;38:71–6.

26 Davis ID, Quirk J, Morris L, *et al*. A pilot study of peripheral blood BDCA-1 (CD1c) positive dendritic cells pulsed with NY-ESO-1 ISCOMATRIX adjuvant. *Immunotherapy* 2017;9:249–59.

27 Tselikas L, Dardenne A, de Baere T, *et al*. Feasibility, safety and efficacy of human intra-tumoral immuno-therapy. Gustave Roussy's initial experience with its first 100 patients. *Eur J Cancer* 2022;172:1–12.

28 Chesney JA, Ribas A, Long GV, *et al*. Global phase III trial of talimogene laherparepvec combined with pembrolizumab for advanced melanoma. *J Clin Oncol* 2023;41:528–40.

29 Schwarze JK, Awada G, Cras L, *et al*. Intratumoral combinatorial administration of CD1c (BDCA-1)(+) myeloid dendritic cells plus Ipilimumab and avelumab in combination with intravenous low-dose nivolumab in patients with advanced solid tumors: a phase IB clinical trial. *Vaccines (Basel)* 2020;8:670.

30 Schwarze JK, Tijtgat J, Awada G, *et al*. Intratumoral administration of CD1c (BDCA-1)(+) and CD141 (BDCA-3)(+) myeloid dendritic cells in combination with talimogene laherparepvec in immune checkpoint blockade refractory advanced melanoma patients: a phase I clinical trial. *J Immunother Cancer* 2022;10:e005141.

31 Didierlaurent AM, Laupèze B, Di Pasquale A, *et al*. Adjuvant system AS01: helping to overcome the challenges of modern vaccines. *Expert Rev Vaccines* 2017;16:55–63.

32 Bosteels C, Fierens K, De Prijck S, *et al*. CCR2- and Flt3-dependent inflammatory conventional type 2 dendritic cells are necessary for the induction of adaptive immunity by the human vaccine adjuvant system AS01. *Front Immunol* 2020;11:606805.

33 Livingston PO, Adluri S, Helling F, *et al*. Phase 1 trial of immunological adjuvant QS-21 with a GM2 Ganglioside-keyhole limpet haemocyanin conjugate vaccine in patients with malignant melanoma. *Vaccine* 1994;12:1275–80.

34 Coccia M, Collignon C, Hervé C, *et al*. Cellular and molecular synergy in AS01-adjuvanted vaccines results in an early Ifngamma response promoting vaccine immunogenicity. *NPJ Vaccines* 2017;2:25.

35 McGirr A, Widenmaier R, Curran D, *et al*. The comparative efficacy and safety of herpes zoster vaccines: a network meta-analysis. *Vaccine* 2019;37:2896–909.

36 Kreutmair S, Pfeifer D, Waterhouse M, *et al*. First-in-human study of WT1 recombinant protein vaccination in elderly patients with AML in remission: a single-center experience. *Cancer Immunol Immunother* 2022;71:2913–28.

37 Wen PY, Reardon DA, Forst DA, *et al*. Evaluation of GM-CSF and AS01B adjuvants in a phase I/IIa trial of a therapeutic CMV vaccine (VBI-1901) against recurrent glioblastoma (GBM). *JCO* 2021;39:2047.

38 Burny W, Marchant A, Hervé C, *et al*. Inflammatory parameters associated with systemic reactogenicity following vaccination with adjuvanted hepatitis B vaccines in humans. *Vaccine* 2019;37:2004–15.

39 Ho NI, Huis In 't Veld LGM, van Eck van der Sluijs J, *et al*. Saponin-based adjuvants enhance antigen cross-presentation in human CD11c(+) CD1c(+) CD5(-) CD163(+) conventional type 2 dendritic cells. *J Immunother Cancer* 2023;11:e007082.

40 Champiat S, Tselikas L, Farhane S, *et al*. Intratumoral Immunotherapy: from trial design to clinical practice. *Clin Cancer Res* 2021;27:665–79.

41 Lecoultre M, Dutoit V, Walker PR. Phagocytic function of tumor-associated macrophages as a key determinant of tumor progression control: a review. *J Immunother Cancer* 2020;8:001408.

42 Xiao G, Wang K, Wang Z, *et al*. Machine learning-based identification of SOX10 as an immune regulator of macrophage in gliomas. *Front Immunol* 2022;13:1007461.

43 Awada G, Schwarze JK, Tijtgat J. A phase 2 clinical trial of trametinib and low-dose dabrafenib in patients with advanced pretreated NRAS(Q61R/K/L). *Cancers (Basel)* 2021;13.